

Innovative concepts in the DTT neutral beam injector

*Original*

Innovative concepts in the DTT neutral beam injector / Agostinetti, P.; Benedetti, E.; Bonifetto, R.; Bonesso, M.; Calabrò, G.; Cavenago, M.; Crisanti, F.; Dal Bello, S.; Dalla Palma, M.; D'Ambrosio, D.; Dima, R.; Favero, G.; Ferro, A.; Fincato, M.; Grando, L.; Granucci, G.; Lombroni, R.; Marsilio, R.; Murari, A.; Patton, T.; Pepato, A.; Pilan, N.; Raffaelli, F.; Rebesan, P.; Recchia, M.; Ripani, M.; Romano, A.; Sartori, E.; Scarpari, M.; Variale, V.; Ventura, G.; Veronese, F.; Zanino, R.; Zappatore, A.; Zavarise, G.. - In: IEEE TRANSACTIONS ON PLASMA SCIENCE. - ISSN 0093-3813. - STAMPA - 52:9(2024), pp. 3802-3808. [10.1109/TPS.2024.3418133]

*Availability:*

This version is available at: 11583/2994567 since: 2025-05-06T10:46:16Z

*Publisher:*

IEEE

*Published*

DOI:10.1109/TPS.2024.3418133

*Terms of use:*

This article is made available under terms and conditions as specified in the corresponding bibliographic description in the repository

*Publisher copyright*

(Article begins on next page)

ID:

# Innovative concepts in the DTT Neutral Beam Injector

P. Agostinetti<sup>a,b</sup>, E. Benedetti<sup>c</sup>, R. Bonifetto<sup>d</sup>, M. Bonesso<sup>e,f</sup>, G. Calabrò<sup>g</sup>, M. Cavenago<sup>h</sup>, F. Crisanti<sup>g</sup>, S. Dal Bello<sup>a</sup>, M. Dalla Palma<sup>a,b</sup>, D. D'Ambrosio<sup>i</sup>, R. Dima<sup>e</sup>, G. Favero<sup>e,j</sup>, A. Ferro<sup>a</sup>, M. Fincato<sup>a</sup>, L. Grando<sup>a</sup>, G. Granucci<sup>k</sup>, R. Lombroni<sup>g</sup>, R. Marsilio<sup>i</sup>, A. Murari<sup>a,b</sup>, T. Patton<sup>a</sup>, A. Pepato<sup>e</sup>, F. Raffaelli<sup>c</sup>, P. Rebesan<sup>e</sup>, M. Recchia<sup>a,b</sup>, M. Ripani<sup>l</sup>, A. Romano<sup>m,n</sup>, E. Sartori<sup>a,j</sup>, M. Scarpari<sup>g</sup>, V. Variale<sup>o</sup>, G. Ventura<sup>p</sup>, F. Veronese<sup>a</sup>, R. Zanino<sup>d</sup>, A. Zappatore<sup>d</sup>, G. Zavarise<sup>p</sup>

<sup>a</sup>Consorzio RFX (CNR, ENEA, INFN, Università di Padova, Acciaierie Venete SpA), Corso Stati Uniti 4, 35127 Padova, Italy

<sup>b</sup>CNR-Institute for Plasma Science and Technology-Section of Padova, Corso Stati Uniti 4, 35127 Padova, Italy

<sup>c</sup>INFN-Section of Pisa - Polo Fibonacci, Largo B. Pontecorvo 3, 56127 Pisa, Italy

<sup>d</sup>NEMO Group, Energy Department, Politecnico di Torino, C.so Duca degli Abruzzi 24, 10129 Torino, Italy

<sup>e</sup>INFN-Section of Padova, Via Marzolo 8, 35131 Padova, Italy

<sup>f</sup>Dept. of Industrial Engineering, University of Padova, Via Marzolo 9, 35131 Padova, Italy

<sup>g</sup>Dept. of Economics, Engineering, Society and Business Organization, University of Tuscia, Largo dell'Università, 01100 Viterbo, Italy

<sup>h</sup>INFN-LNL, v.le dell'Università 2, I-35020, Legnaro (PD), Italy

<sup>i</sup>Dept. of Mechanical and Aerospace Engineering, Politecnico di Torino, C.so Duca degli Abruzzi 24, 10129 Torino, Italy

<sup>j</sup>Dept. of Management and Engineering, University of Padova, Strad. S. Nicola 3, 36100 Vicenza, Italy

<sup>k</sup>CNR-Institute for Plasma Science and Technology-Section of Milano, Via R. Cozzi 53, 20125 Milano, Italy

<sup>l</sup>INFN-Section of Genova, Via Dodecaneso 33, 16146 Genova, Italy

<sup>m</sup>ENEA, Fusion and Nuclear Safety Department, C.R. Frascati, Via E. Fermi 45, 00044 Frascati (Roma), Italy

<sup>n</sup>DTT S.c.a.r.l., Consorzio per l'attuazione del Progetto Divertor Tokamak Test, v. E.Fermi 45, 00044 Frascati (Roma), Italy

<sup>o</sup>INFN-Section of Bari, Via G. Amendola 173, 70126 Bari, Italy

<sup>p</sup>Dept. of Structural, Geotechnical and Building Engineering, Politecnico di Torino, C.so Duca degli Abruzzi 24, 10129 Torino, Italy

[piero.agostinetti@igi.cnr.it](mailto:piero.agostinetti@igi.cnr.it)

**Abstract**— The main purpose of the Divertor Tokamak Test facility (DTT) is to study alternative solutions to mitigate the issue of the power exhaust, under integrated physics and technical conditions relevant to ITER and DEMO. One of the most complex and innovative subsystems of the entire project is certainly the negative-ion-based Neutral Beam Injector (NBI), meant to inject 10 MW of auxiliary power with a beam of 510 keV deuterium neutrals. This contribution describes the conceptual design of the beamline for the DTT NBI system, with a particular focus on the innovative technical solutions adopted to fulfill the requirements and maximize the performance.

The DTT NBI is required to operate with high efficiency in several operating scenarios, covering a large range of beam energies, between 10% and 100% of the nominal value (510 keV). To reach this challenging goal, an innovative accelerator design, the Spherical and Lemon Hyperlens Grids (SLHG), has been developed. The implementation of this design concept of the accelerator has recently become possible thanks to recent improvements of the additive manufacturing technology.

Another original aspect of the DTT NBI, compared to existing devices, regards the vacuum pumping system, which will be based on Non-Evaporable Getter (NEG) pumps. This will represent the first application of the NEG technology to an NBI for the heating and current drive system of a fusion experiment, with a possible simplification of the overall construction, with respect to typical solutions based on cryogenic pumps.

Other innovative solutions are the Cylindrical Sawtooth Structure (CSS) for the neutralizer panels and the Stray Field Shielding System (SFSS) with encapsulated neutralizer.

This paper provides an overview of the injector for DTT NBI with a particular focus on the innovative technical solutions.

**Index Terms**— DTT, NBI, neutral, beam, injector

## I. INTRODUCTION

THE main purpose of the Divertor Tokamak Test facility (DTT) [1] is to study solutions to mitigate the issue of power exhaust in conditions relevant for ITER and the European DEMO, aiming at developing power exhaust solutions suitable for the machines that will follow ITER [2][3], in particular the demonstration power plant DEMO that is currently in the conceptual design phase [4].

In this context, the principal objective of DTT is to mitigate the risk that exists if one has to extrapolate from a conventional divertor based on detached conditions, as it will be tested in ITER, to a fusion reactor that most likely has to use an alternative divertor configuration. The task implies the study of completely integrated power exhaust problems and the demonstration of how the possible implemented solutions (e.g., advanced divertor configurations or liquid metals) could be integrated in the DEMO device and other fusion reactors.

DTT will be able to explore various magnetic divertor configurations and, in order to reach a reactor relevant power flow to the divertor, 45 MW of auxiliary power will have to be

ID:

coupled to the plasma using the following heating systems: Electron Cyclotron Resonant Heating (ECRH), Ion Cyclotron Resonant Heating (ICRH) and Neutral Beam Heating (NBH) [5].

In this framework, an overview of the conceptual design of the beamline for the DTT NBH system, based on negative ions, is presented, with a particular focus on the innovations adopted to fulfill the requirements and maximize beamline performance.

## II. DESIGN DESCRIPTION

The proposed system features a beamline providing deuterium neutrals ( $D^0$ ) with an energy of 510 keV and an injected power of 10 MW. Regarding the effect of the NBI in DTT, recent studies are reported in [6], [7] and [8].

An overview of the current conceptual design of the beamline for the DTT Neutral Beam Injector (NBI) is given in Fig. 1, while Tab. 1 reports the main functional parameters.

Parameter	Value
Injected power	10 MW
Beam Energy	510 keV
Accelerated $D^-$ current	40 A
Extracted $D^-$ current density	$> 239 \text{ A m}^{-2}$
Ion source filling pressure	$\geq 0.3 \text{ Pa}$
Extracted current uniformity	$\pm 10\%$
Beam on time	50 s
Co-extracted electron fraction ( $e^-/D^-$ )	$< 1$
Beamlet divergence	$< 7 \text{ mrad}$
Auxiliaries/extraction efficiency <sup>a</sup>	0.9
Accelerator efficiency <sup>b</sup>	0.8
Beam source/neutralizer entrance transmission efficiency <sup>c</sup>	0.95
Neutralizer efficiency <sup>d</sup>	0.55
Beam line/duct transmission efficiency <sup>e</sup>	0.95

Tab. 1 - Main functional parameters of the DTT NBI. <sup>a</sup> total power absorbed by the accelerator divided by the total power consumption of the accelerator power supplies plus the auxiliaries of the NBI system; <sup>b</sup> ion beam power at the exit of the accelerator divided by the theoretical ion beam power without stripping losses and interception of halo on the grids; <sup>c</sup> ion beam power at the entrance of the neutralizer divided by the ion beam power at the exit of the accelerator; <sup>d</sup> neutral beam power at the exit of the neutralizer divided by the ion beam power at the entrance of the neutralizer; <sup>e</sup> neutral beam power reaching the main chamber divided by the neutral beam power at the exit of the neutralizer.

Similarly to the NBIs of JT60 [9] and LHD [10], a design with an air-insulated beam source is adopted for DTT NBI, i.e. the accelerator and ion source assemblies are connected to the rear part of the vacuum vessel, as shown in Fig. 1a. This solution was selected because it maximizes the Reliability and Availability indices (evaluated as in [11]), by improving the beam source accessibility and simplifying the design. The DTT NBI design differs from the Japanese scheme in the choice of the ion source: in fact, it is proposed to use the same Radio Frequency source concept adopted for ITER, mainly developed by IPP Garching [11]. The Beam Line Components (BLC), i.e. the Neutralizer, the Residual Ion Dump (RID) and the Calorimeter, will be ITER-like too, whereas the vacuum vessel will not include any large flanges (differently from ITER) to reduce cost and weight of the vessel.

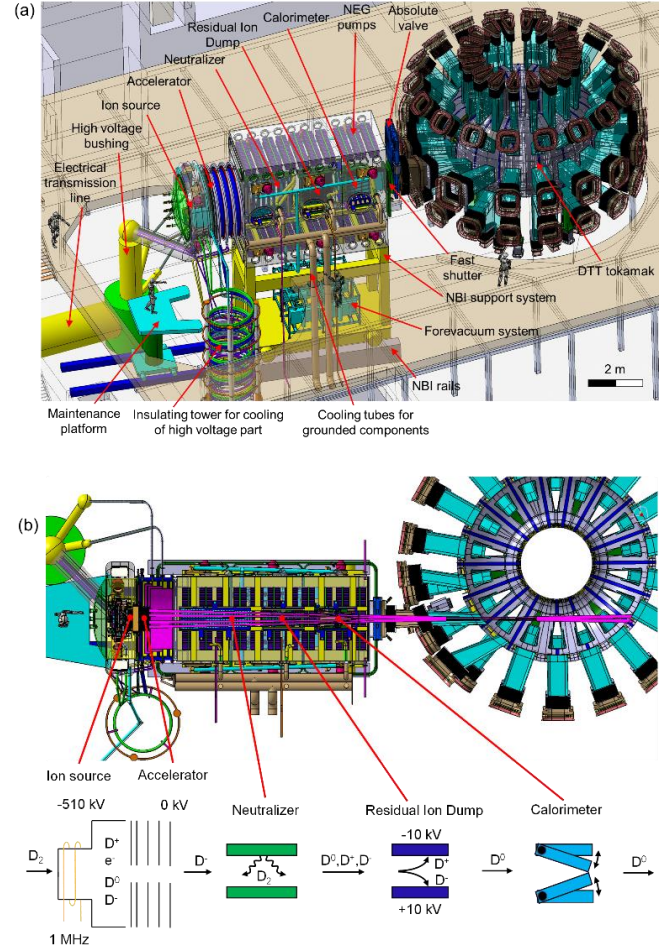


Fig. 1. Overview of the DTT NBI conceptual design: (a) overall injector view with connections to external auxiliary systems; (b) top view with functional scheme.

Small flanges are foreseen on the lateral walls of the vacuum vessel for pumping, diagnostics and supply lines to the BLCs, while the access for BLCs maintenance is planned to be from the large circular flange of the accelerator, after removing the ion source and accelerator. Dedicated rails are hosted inside the vacuum vessel to insert and extract the BLCs, and to support them when they are in operating position. The maintenance of the ion source and accelerator will be carried out using a dedicated maintenance platform (shown in Fig. 1a), able to reach the critical regions of these components.

A transmission line and an insulating tower will be located at the two sides of the ion source, as shown in Fig. 1a. The transmission line will bring the electrical power to the ion source and accelerator through a high voltage bushing connected to the ion source at -510 kV, and two smaller bushings biasing the two acceleration grids. The insulating tower will provide the cooling water to the ion source and accelerator. To reduce the drain current between high voltage components and ground to acceptable values, the insulating tower will feature plastic tubes wound like spirals.

Also the tubes bringing the deuterium gas to the ion source and the pipes for the exhaust system of the high voltage vacuum system will pass through the insulating tower, as they are also

ID:

connecting components at high voltage (-510 kV) with the ground.

A section view of the whole injector with a functional scheme is shown in Fig. 1b. More information on the functions of the various components of the injector are reported in [13].

### III. INNOVATION 1: SPHERICAL AND LEMON HYPERLENS GRIDS (SLHG) AIMING CONCEPT

In DTT NBI, the aiming strategy adopted for DTT is the multi focus concept, the same adopted for ITER HNB and MITICA [14], where the horizontal and vertical focus points of the beamlets are separated, as shown in Fig. 2a. In fact the horizontal focus of each beam blade is located at the exit of the Residual Ion Dump (RID), while the vertical focus is inside the plasma in the tokamak, about 200 mm downstream of the first wall. This setup reduces the beam cross-section in the region of the Neutralizer and RID, leading to reduced losses by impingement due to ill-focused particles, while not increasing excessively the beam footprint on the plasma in the tokamak.

To do this, the Hyperlens Grid (HG) concept was previously presented [15], which consists of additional grids placed downstream of the main ones and having a lens-like profile, tailored to apply the desired aiming to the beamlets. Although providing optimal beam optics, the main issue with this approach resides in the extremely complex machining process that would be required in order to manufacture the HGs.

Hence, another concept called Spherical and Lemon Hyperlens Grids (SLHG) [16] has been developed as an evolution of the HG concept. The name Lemon is the mathematical term used to refer to a geometric shape that is constructed as the surface of revolution of a circular arc rotated about an axis passing through the endpoints of the arc.

The main reason to switch from the HG to the SLHG concept was related to the manufacturing. In fact, the choice of AM as the manufacturing technology for the grids has allowed adopting a spherical shape for the main grids, providing acceleration and part of the aiming thanks to their curvature. This technology also allows to manufacture the two-curvature, continuous lens-like grids, called the Lemon Hyperlens Grids, dedicated to the aiming of each of the four beam blades.

By performing several sets of multibeamlet simulations in COMSOL (see Fig. 2b for an example), the SLHG design solution has been found to provide excellent beam optics in the reference operating scenario (see Fig. 2c) and also good ones in out of reference scenarios (for example, with a half energy beam), with a significant improvement with respect to the previous design solutions. From Fig. 3c, where the stars show the intersection of the beamlet trajectory axes with the GG exit plane while the arrows show the perpendicular velocity component with a convenient scaling, it can be observed that the calculated and ideal trajectories are almost coincident (in fact, blue and red points and arrows almost perfectly overlap), meaning excellent beam optics. Detailed information on this topic can be found in [16].

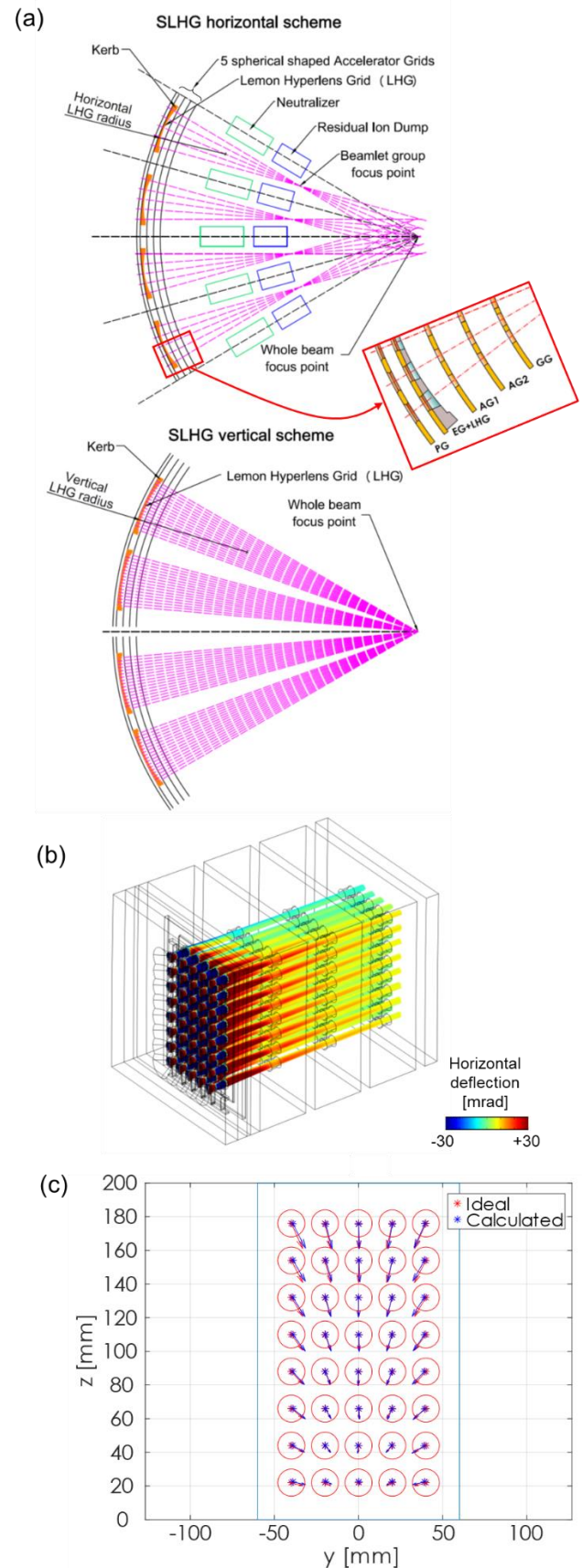


**Fig. 2.** SLHG concept: (a) SLHG aiming schematic as adopted in DTT NBI; (b) example of a trajectory simulation; (c) comparison between ideal trajectories (in red) and calculated deflections (in blue).

ID:

#### IV. INNOVATION 2: APPLICATION OF ADDITIVE MANUFACTURING TO ACCELERATOR GRIDS

Strictly related to the first innovation regarding the grid shape is the second innovation here described, that provides a technology able to produce these grids, i.e. the Additive Manufacturing (AM) process.

AM permits to generate complex shapes like the ones foreseen with the spherical and lemon-shaped grids described in the previous section. In fact, this technology allows producing a more sophisticated design not only of the grids but also of the cooling channels inside them, with a consequent advantage in terms of cooling effect. This last point is crucial as the grids are subjected to very high and concentrated heat loads due to the particles generated and accelerated inside the accelerator.

An important R&D program, to develop and optimize the AM process for the grids of DTT NBI, is ongoing at the INFN laboratories of Padova. Some recent prototypes are shown in Fig. 3.

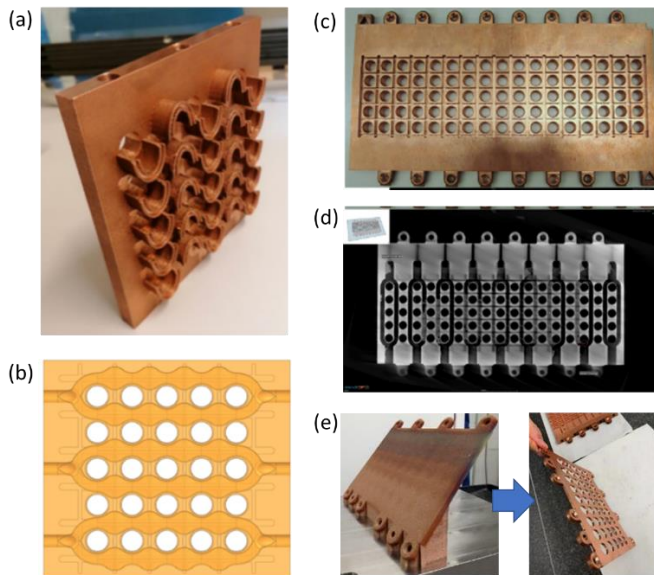


**Fig. 3.** R&D on additive manufacturing applied to the accelerator grids of DTT NBI: (a) power test prototype in CuCrZr alloy; (b) cooling channels layout of the power test prototype; (c) Extraction Grid prototype; (d) check of internal channels using tomography; (e) Lemon Hyperlens Grid prototype.

The R&D process started using pure copper with different granulometry using a low laser power (<370 W) AM machine with infrared wavelength [16]. The research then continued exploring the CuCrZr alloy, which was proven to be a good substitute to pure copper due to its superior mechanical properties without losing too much in terms of thermal conductivity. Subsequently, machines with high power infrared and green lasers equipped with building chambers that can allocate full scale prototypes have been tested. The most promising combinations of materials and machines tested so far are reported in Tab. 2, together with the main material properties measured on the samples.

		1 kW Infrared <b>Pure copper</b>	1 kW Infrared <b>CuCrZr</b>	1 kW Green <b>Pure copper</b>
Porosity Archimedes		0.38 %	0.63 %	1.02 %
Thermal conductivity [W/m K]	H	375 ± 19	300 ± 15	370 ± 19
	V	376 ± 19	323 ± 16	374 ± 19
Yield Strength [MPa]	H	159.3 ± 0.6	199.3 ± 4.7	140.3 ± 1.5
	V	161.7 ± 1.2	169.3 ± 27.0	142.3 ± 3.8
Ultimate Tensile Strength [MPa]	H	225.9 ± 0.1	340.9 ± 3.0	211.6 ± 4.1
	V	224.9 ± 0.6	283.3 ± 20.5	192.7 ± 4.8
Young's Module [GPa]	H	117.1 ± 7.02	128.2 ± 0.6	112.8 ± 4.5
	V	126.6 ± 4.16	106.3 ± 3.5	112.1 ± 5.9

Tab. 2 - Material characterization of pure Cu and CuCrZr alloy produced via different AM machines. The thermo-mechanical properties were tested at vertical (V) and horizontal (H) orientations.

In parallel, the design of the cooling channel has been optimized through Computational Fluid Dynamics (CFD) simulations and experimental tests [18] and the post-process chemical polishing of the internal wall of the cooling channels has been tuned to reach a surface roughness of  $\sim 1 \mu\text{m}$  [19].

The overall results led to the manufacturing of several grid prototypes by means of AM. First, power test prototypes with 5x5 beamlets and 6 cooling channels in parallel were manufactured using the three materials analyzed in Tab. 2. These prototypes have extrusions, shown in Fig. 3a, that aim at reproducing the heat flux map similarly with the beam optics simulation results.

Other prototypes, as shown in Fig. 3c and Fig. 3e, have been manufactured to test other post process operations and to measure the final dimensional accuracy of the parts. The post-process operations that are being currently studied are the heat treatment of the CuCrZr alloy, the milling of the external surfaces and the grooves for the magnets, and the electron beam welding of the components.

Finally, full-scale AM grids prototypes have been manufactured using the CuCrZr alloy.

#### V. INNOVATION 3: FIRST APPLICATION OF NEG TO AN NBI

Non-Evaporable Getter pumps have recently reached a level of performance [20] that make them a good alternative to cryopumps for neutral beam injectors, with some additional advantages related to the fact that they work at room temperature. For this reason, in DTT NBI for the first time a vacuum system based on NEG pumps will be implemented for a full neutral beam injector [21].

ID:

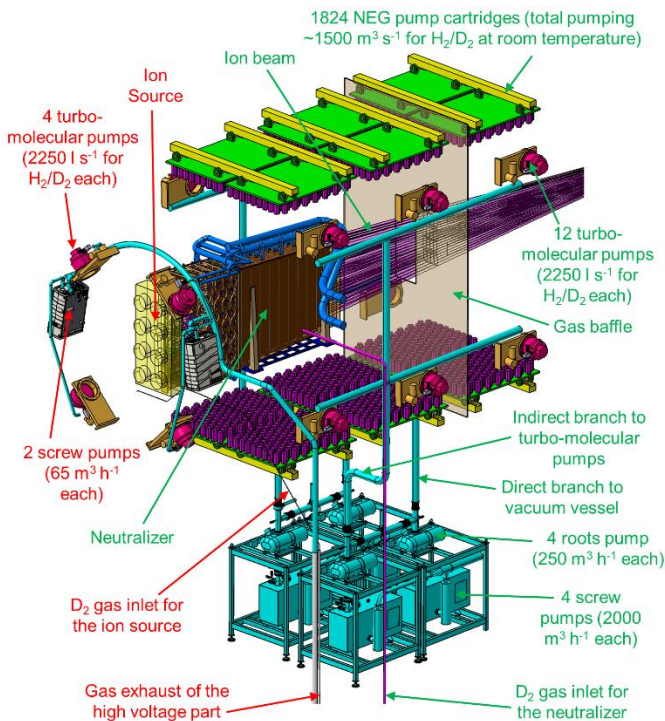


**Fig. 4.** Conceptual design of the Gas Injection and Vacuum System (GVS) for DTT NBI

The Gas injection and Vacuum System (GVS) for the DTT NBI will be composed of two parts:

- A grounded section connected to the main vacuum vessel (green legends in Fig. 4). This part is made of a fore-vacuum system (given by 4 screw pumps and 4 roots pumps) plus a UHV system based on 12 turbo-molecular pumps, located on the side walls of the vessel, and Non-Evaporable Getter (NEG) pumps, located inside the vessel on the upper and lower surfaces.
- A high voltage part connected to the ion source vessel and working at -510 kV voltage (red legends in Fig. 4). This part consists of a fore-vacuum system (given by two compact screw pumps mounted on the external surface of the ion source vessel) plus a UHV system based on 4 turbo-molecular pumps, also located on the side walls of the ion source vessel.

The design of the fore-vacuum group and turbopumps group for DTT NBI benefits from the R&D and manufacturing experience coming from SPIDER and MITICA [22], while the NEG part has been developed in collaboration with industry.

The operation of a NEG pump foresees cycles with two subsequent phases:

- A sorption phase (with temperature  $< 150$  °C), when the getter material absorbs the gas in the material structure.
- A reactivation (or regeneration) phase (with temperature  $> 450$  °C), when the getter material

releases the hydrogen in the vacuum while the other gases diffuse into the material structure.

The main advantages of NEG compared to cryopumps are that they can work at room temperature without any supply and no cryogenic plant is needed. A drawback is that high temperatures are needed during regeneration, hence the components inside the vessel must be protected to avoid excessive heating.

More detailed information on NEG pumps for fusion application are reported in [20], while an elaborate description of the GVS for DTT NBI can be found in [21].

#### VI. INNOVATION 4: NEUTRALIZER PANELS WITH CYLINDRICAL SAWTOOTH STRUCTURE (CSS)

The typical neutralizers for neutral particle injectors currently consist of an open chamber in which a certain gas density is imposed in order to maximize the fraction of neutral particles exiting the neutralizer. Indeed, only neutral particles are able to reach the plasma inside the main chamber in order to heat it. For the particle beam to pass through, the chamber must necessarily be open at the inlet and outlet sections. To be able to achieve the required gas density while minimizing the gas flow to the outside of the neutralizer, where vacuum pumps are mounted to absorb this gas flow. Minimizing the conductance of the neutralizer is crucial to achieve an acceptable gas flow for the vacuum pumps (this has a significant impact on injector costs) and a sufficiently low density in the vessel area outside the neutralizer (this has a significant impact on the injector efficiency).

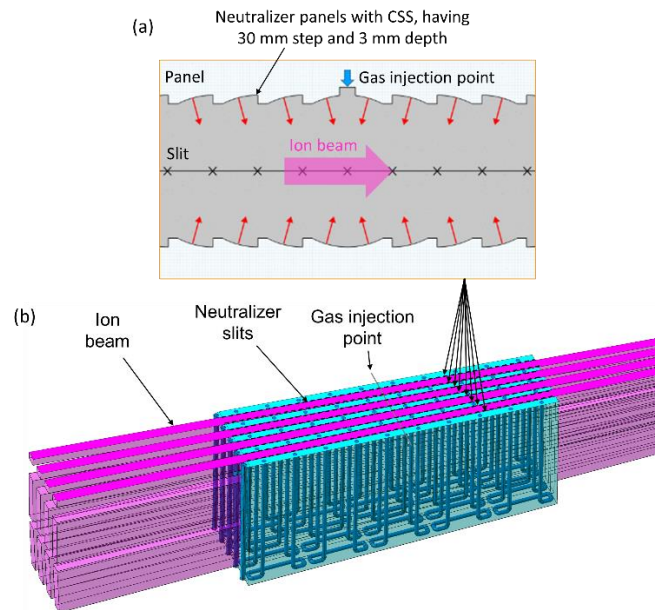


**Fig. 5.** Neutralizer panels with Cylindrical Sawtooth Structure (CSS): (a) CSS applied to the DTT NBI neutralizer; (b) section view of the neutralizer.

To further minimize the conductance, in addition to the slitted shape of the neutralizer, the Cylindrical Sawtooth Surface concept has been considered in the DTT NBI. This concept is based on the introduction of a deliberate roughness profile within the main direction of each slit, of size comparable to a

ID:

fraction the channel width, following the results of observations of molecular flow in similar setups [23][24]: when channel roughness is regular (e.g. with a sawtooth profile) and under around 10% of the channel width (so that the channel is still macroscopically “flat”), the transmission probability of a given particle is lower than the expected value for an equivalent-sized smooth channel.

In the presence of a density gradient, this introduced roughness favors systematically the likeliness of a “upstream” diffusion. In our context of gas flow from a central nozzle in a slit configuration, this may be interpreted as particles having their free path toward the exit shadowed by the channel roughness, more often returning towards the center, while still macroscopically flowing outside. The result is a shorter average mean free path, and an increased average density for the same gas throughput, i.e. a reduced conductance.

The CSS geometry, shown in Fig. 5, is the result of the adoption and rough optimization of a first guess profile based on arcs and straight edges. This profile is also a compromise in size between a smaller roughness and obtaining a bulkier component capable of withstanding the local heat load caused by impinging fast beam particles, that would otherwise flatten in due time an otherwise more delicate profile etched in the neutralizer panels.

A numerical comparison of the traditional solution with smooth walls and that with CSS geometry shows that, for the same flux, the average gas density inside the neutralizer remains significantly higher in the CSS case.

In DTT NBI, this solution should allow to reduce the gas flow by up to 34% in order to achieve the same average density (required for efficient neutralization of the ion beam), which implies a significant advantage in terms of pumping system cost and injector efficiency.

R&D activities are on-going to look further into the choice of possible roughness profiles, to check the possible concentration of the heating power on the neutralizer panels due to the shape of the panels, to choose to most suitable manufacturing process and estimate the related costs.

## VII. INNOVATION 5: ENCAPSULATED NEUTRALIZER

As the DTT NBI is quite close to the tokamak, the NBI region is interested by a strong stray poloidal field that, if not compensated, would be detrimental for the optics of the negative ions, especially in the accelerator and neutralizer region, reducing the overall efficiency of the NBI system and increasing the heat loads on the main components. Hence, a Stray Field Shielding System (SFSS) has to be implemented, similarly to the system implemented in ITER NBI [25] and W7X NBI [26].

After a comparison among different design solutions [27], the design option featuring a fully passive ferromagnetic shield encapsulating the neutralizer (shown in Fig. 6a) has been chosen for the SFSS. Heat loads from the accelerated electrons are expected on the region of the ferromagnetic shield between the grounded grid and the neutralizer (see Fig. 6b) hence a dedicated cooling system is being implemented on the shield to keep its temperature controlled.

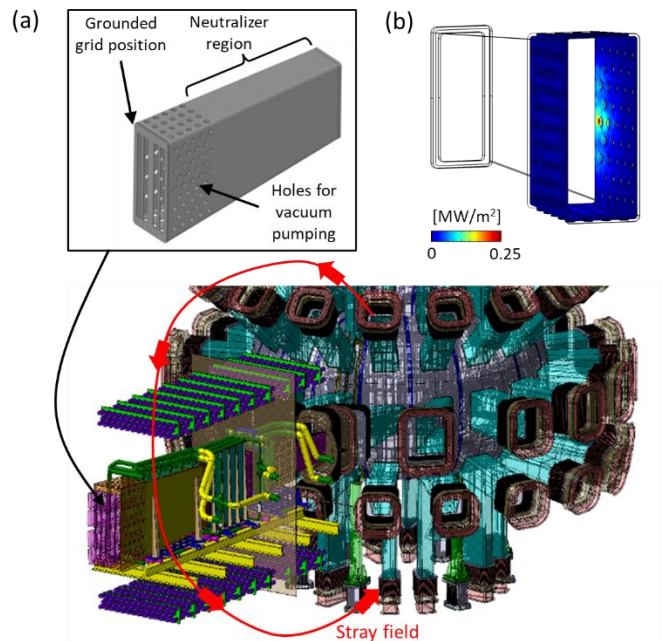


**Fig. 6.** Stray Field Shielding System (SFSS) for DTT NBI: (a) conceptual design showing the neutralizer encapsulated by a ferromagnetic shield, without any active coil; (b) heat load power density expected by the electrons on the region of the ferromagnetic shield between the grounded grid and the neutralizer.

The SFSS concept chosen for DTT is completely passive, meaning absence of any coil with related control system and power supplies, and completely internal, meaning less iron and less issues related to the interfaces with the components located outside the vessel, like the diagnostic systems, cooling pipes, electrical connections, gas inlets etc. On the other hand, a critical aspect of this design solution is related to its effect on the vacuum pumping system. In fact, the presence of the SFSS in the region between the grounded grid and neutralizer decreases the vacuum pumping efficiency in that region. This detrimental effect is minimized by adding a suitable set of holes in that part of the shield, as shown in Fig. 6a.

Simulations are on-going to optimize the design of the SFSS in order to find the most suitable compromise between magnetic shielding capability and low impact on the vacuum pumping system, by choosing the most suitable shield thickness and features of the holes in terms of number, diameter and position.

## VI. CONCLUSIONS

The conceptual design of the injector for the DTT NBI system is being developed considering 510 keV beam energy and 10 MW injected to the plasma.

Several innovative technical solutions are under development to maximize the performance of the NBI, increase its RAMI indices and decrease its cost.

Comprehensive R&D programs are on-going regarding these innovative aspects and will continue in the next years, when the DTT NBI project will enter in the engineering design phase.

ID:

#### ACKNOWLEDGEMENTS

This work has been carried out within the framework of the EUROfusion Consortium, funded by the European Union via the Euratom Research and Training Programme (Grant Agreement No 101052200 — EUROfusion). Views and opinions expressed are however those of the author(s) only and do not necessarily reflect those of the European Union or the European Commission. Neither the European Union nor the European Commission can be held responsible for them.

#### REFERENCES

- [1] R. Ambrosino, et al., “DTT - Divertor Tokamak Test facility: A testbed for DEMO”, *Fusion Eng. Des.* 167 (2021) 112330.
- [2] R. Albanese, et al., “Design review for the Italian Divertor Tokamak Test facility”, *Fusion Eng. Des.* 146 (2019) 194-197.
- [3] G. Mazzitelli, et al., “Role of Italian DTT in the power exhaust implementation strategy”, *Fusion Eng. Des.* 146 (2019) 932-936.
- [4] G. Federici et al., “Overview of the DEMO staged design approach in Europe”, *Nucl. Fusion* 59 (2019) 066013.
- [5] G. Granucci, et al., “The DTT device: System for heating”, *Fusion Eng. Des.* 122 (2017) 349-355.
- [6] G. Spizzo, et al., “Collisionless losses of fast ions in the divertor tokamak test due to toroidal field ripple”, *Nucl. Fusion* 61 (2021) 116016.
- [7] I. Casiraghi, et al., “First principle-based multi-channel integrated modelling in support of the design of the Divertor Tokamak Test facility”, *Nucl. Fusion* 61 (2021) 116068.
- [8] P. Vincenzi et al., “Interaction of high-energy neutral beams with Divertor Tokamak Test plasma”, *Fus. Eng. Des.* 189 (2023) 113436.
- [9] A. Kojima et al., “Progress in long-pulse production of powerful negative ion beams for JT-60SA and ITER”, *Nucl. Fusion* 55 (2015) 063006
- [10] Y. Takeiri et al., “High-power and long-pulse injection with negative-ion-based neutral beam injectors in the Large Helical Device”, *Nucl. Fusion* 46 (2006) S199-S210.
- [11] P. Agostinetti, et al., “RAMI evaluation of the beam source for the DEMO neutral beam injectors”, *Fus. Eng. Des.* 159 (2020) 111628
- [12] B. Heinemann et al., “Latest achievements of the negative ion beam test facility ELISE”, *Fus. Eng. Des.* 136 (2018) 569-574.
- [13] P. Agostinetti, et al., “Improved Conceptual Design of the Beamline for the DTT Neutral Beam Injector”, *IEEE Trans. on Plasma Science*, 50 (2022) 4027-4032.
- [14] P. Agostinetti, et al., “Detailed design optimization of the MITICA negative ion accelerator in view of the ITER NBI”, *Nucl. Fusion* 56 (2016) 016015.
- [15] F. Veronese, et al., “Performance Optimization of the Electrostatic Accelerator for DTT Neutral Beam Injector”, *IEEE Trans. on Plasma Science*, 50 (2022) 4033-4038.
- [16] F. Veronese, et al., “The Lemon Hyperlens concept and its application to the DTT Neutral Beam Injector”, in *IEEE Transactions on Plasma Science*, doi: 10.1109/TPS.2024.3353349
- [17] M. Bonesso, et al., Effect of particle size distribution on laser powder bed fusion manufacturability of copper, *Berg Huettenmaenn Monatsh* 166 (2021) 256–262.
- [18] G. Favero, et al., Additive manufacturing for thermal management applications: from experimental results to numerical modeling, *Int. J. Thermofluids* 10 (2021) 100091.
- [19] G. Favero, et al., Experimental and numerical analyses of fluid flow inside additively manufactured and smoothed cooling channels, *Int. Comm. Heat Mass Trans.* 135 (2022) 106128.
- [20] F. Siviero, et al., Robustness of ZAO based NEG pump solutions for fusion applications, *Fusion Eng. Des.* 166 (2021) 112306.
- [21] P. Agostinetti, et al., “Conceptual design of the Gas Injection and Vacuum System for DTT NBI”, *Fusion Eng. Des.* 192 (2023) 113638.
- [22] S. Dal Bello, et al., “SPIDER gas injection and vacuum system: From design to commissioning”, *Fusion Eng. Des.* 146 (2019) 1485-148
- [23] D. H. Davis, et al., “Effect of ‘Rougher-than-Rough’ Surfaces on Molecular Flow through Short Ducts.” *Journal of Applied Physics* 35, 529 (1964); doi: 10.1063/1.1713407
- [24] O. Sazhin, “The effect of surface roughness on internal free molecular gas flow.” *Vacuum* 159 (2019) 287–292, doi: 10.1016/j.vacuum.2018.09.031
- [25] G. Barrera, et al., “Magnetic analysis of the magnetic field reduction system of the ITER neutral beam injector”, *Fusion Eng. Des.* 96-97 (2015) 400-404.
- [26] M. Kick, et al., “Shielding of the NBI boxes against W7-X magnetic stray fields” , *Fusion Eng. Des.* 84 (2009) 1020–1025.
- [27] F. Veronese, et al., Comparison among possible design solutions for the Stray Field Shielding System of the DTT Neutral Beam Injector, *JINST* 18 (2023) C06018.